

Antileishmanial Evaluation of Bark Methanolic Extract of *Acacia nilotica*: *In Vitro* and *In Silico* Studies

Rahat Ali,[¶] Shams Tabrez,[¶] Fazlur Rahman,[¶] Abdulaziz S. Alouffi, Bader M. Alshehri, Fahdah Ayed Alshammari, Mohammed A. Alaidarous, Saeed Banawas, Abdul Aziz Bin Dukhyil, and Abdur Rub*



Cite This: *ACS Omega* 2021, 6, 8548–8560



Read Online

ACCESS |

 Metrics & More

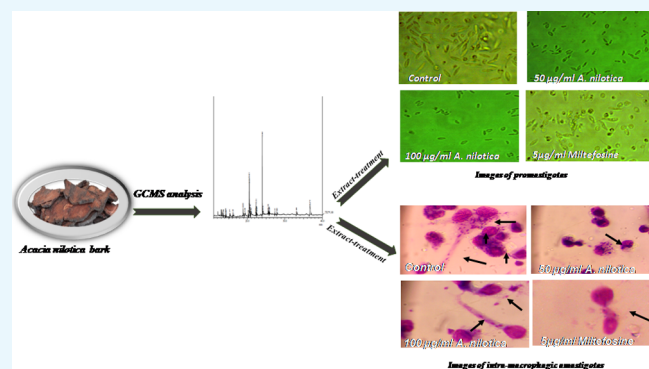


Article Recommendations



Supporting Information

ABSTRACT: *Acacia nilotica* (*A. nilotica*) is an important medicinal plant, found in Africa, the Middle East, and the Indian subcontinent. Every part of the plant possesses a wide array of biologically active and therapeutically important compounds. We reported the antileishmanial activity of *A. nilotica* bark methanolic extract through *in vitro* antileishmanial assays and dissected the mechanism of its action through *in silico* studies. Bark methanolic extract exhibited antipromastigote and antimastigote potential in a time and dose-dependent manner with IC₅₀ values of 19.6 ± 0.9037 and 77.52 ± 5.167 µg/mL, respectively. It showed cytotoxicity on THP-1-derived human macrophages at very high dose with a CC₅₀ value of 432.7 ± 7.71 µg/mL. The major constituents identified by gas chromatography–mass spectrometry (GC–MS) analysis, 13-docosenoic acid, lupeol, 9,12-octadecadienoic acid, and 6-octadecanoic acid, showed effective binding with the potential drug targets of *Leishmania donovani* (*L. donovani*) including sterol 24-c-methyltransferase, trypanothione reductase, pteridine reductase, and adenine phosphoribosyltransferase, suggesting the possible mechanism of its antileishmanial action. Pharmacokinetic studies on major phytoconstituents analyzed by GC–MS supported their use as safe antileishmanial drug candidates. This study proved the antileishmanial potential of bark methanolic extract *A. nilotica* and its mechanism of action through the inhibition of potential drug targets of *L. donovani*.



1. INTRODUCTION

Visceral leishmaniasis (VL), also known as kala-azar in the Indian subcontinent, is a fatal form of the vector-borne disease caused by protozoan parasite *Leishmania donovani*. The disease remained endemic in more than 88 countries around the globe, while 95% of cases are concentrated in 7–8 countries.¹ More than 50% of the global burden of VL is found in the Indian subcontinent (India, Bangladesh, and Nepal).^{2,3} The disease is proved to be fatal if left untreated in more than 95% of cases because of secondary infection and anemia.⁴ VL is ranked second in the mortality rate among the neglected tropical diseases.^{5,6} It is a significant problem for the economically weaker section of the society. Due to their unhygienic living environment, they are more vulnerable to the disease.⁷ Illiteracy is another factor that is directly proportional to the lack of awareness which led to major morbidity and mortality. The available chemotherapy of VL is limited and undermined by drug resistance. Currently, in general, the drug used in the Indian subcontinent sodium antimony gluconate showed no response in more than 64% of the patients due to the development of resistance against the parasites.⁸ Miltefosine, amphotericin B, and its lipid formulations have several

limitations because of high toxicity, cost, and unavailability, which limit their use. The present scenario of disease and its limited treatment options demand an urgent need to develop a promising and cost-effective operational drug to overcome the disease. To date, a large number of medicinal plants and their extracts had been studied for antileishmanial activity and proved to be potential therapeutic options.^{9,10} Here, we planned to explore the antileishmanial activity of the medicinal plant, *Acacia nilotica*. *A. nilotica* is commonly known as babul and belongs to the family Fabaceae of genus *Acacia*. It is an important medicinal plant, found in Africa, the Middle East, and the Indian subcontinent.^{11–13} It is rich in secondary metabolites including condensed tannins, flavonoids, gums, and phlobatannins.^{14,15} Every part of the plant possesses a wide array of biologically active, therapeutically potential com-

Received: January 20, 2021

Accepted: March 10, 2021

Published: March 18, 2021



ACS Publications

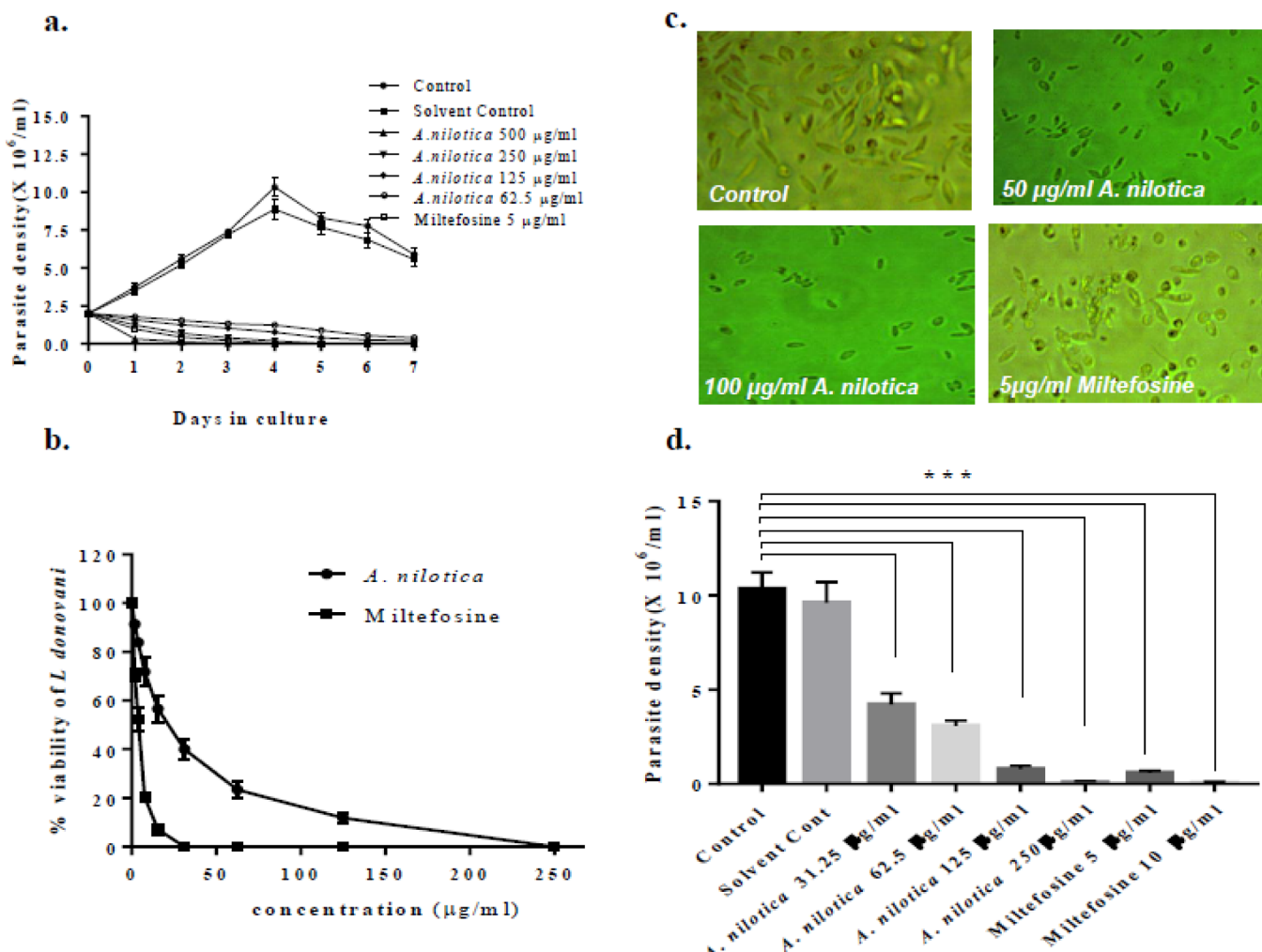


Figure 1. *A. nilotica* bark methanolic extract inhibited the growth and proliferation of *L. donovani* promastigotes. (a) 2×10^6 stationary phase *L. donovani* promastigotes were treated with different concentrations of *A. nilotica* methanolic plant extracts, with miltefosine as the standard drug and control (without any treatment). (b) 2×10^6 stationary phase *L. donovani* promastigotes were treated with different concentrations of the *A. nilotica* methanolic plant extract fraction and miltefosine; IC_{50} was determined as described in the Materials and Methods. Each point represented the mean \pm SE of the samples in triplicate. (c) Images of the promastigote showing changes in morphology upon extract and miltefosine treatment. (d) Stationary phase *L. donovani* promastigotes were incubated with different concentrations of *A. nilotica*, with miltefosine and DMSO (solvent control). Also, the growth reversal was analyzed as described in Materials and Methods. *** $P < 0.001$ with respect to the parasite control. Antipromastigote efficacy of *A. nilotica* fractions.

pounds that are used in the traditional system of medicine as a remedy for various diseases. Its different parts are used in the treatment of different diseases such as floral parts for gastrointestinal disorders,¹⁶ leaf extracts for cancer and microbial infections,^{17,18} root extracts for tuberculosis and liver disorders,¹⁹ and bark for bacterial infections including cold, bronchitis, dysentery, biliousness, cholera, and bleeding piles.^{14,20–22} Keeping the rich antimicrobial bioactive collection of the bark of *A. nilotica*, in mind, we planned to study its antileishmanial potential here. We also tried to dissect the mechanism of its antileishmanial action through different *in silico* approaches. Sterol 24-c-methyltransferase (SMT), trypanothione reductase (TR), pteridine reductase (PTR1), and adenine phosphoribosyltransferase (APRT) are prerequisite enzymes for survival, pathogenicity, and transmission of *L. donovani*. Therefore, we selected these potential drug targets for the molecular docking study of major constituents of bark extract identified by gas chromatography–mass spectrometry

(GC–MS), with these mentioned potential drug targets of *Leishmania*.

2. RESULTS

2.1. Antileishmanial Activity of *A. nilotica* on *L. donovani* Promastigotes. The growth inhibitory effects of the *A. nilotica* bark methanolic extract fraction were assessed against exponentially growing *L. donovani* promastigotes. *A. nilotica* treatment reduced the promastigote proliferation in a time and dose-dependent manner. Growth kinetics was assessed for 7 days; there was a gradual decrease in the promastigote proliferation at all the doses (Figure 1a). The promastigote culture was completely shattered at the dose concentrations of 250 and 500 $\mu\text{g}/\text{mL}$ of *A. nilotica* after 3 days of treatment. Miltefosine, an established antileishmanial drug, rapidly shattered the promastigote parasites *in vitro*. The *Leishmania* promastigotes, without any treatment or with 0.5% dimethyl sulfoxide (DMSO) (solvent control), exponentially grow till the 4th day of parasite seeding, conforming to no

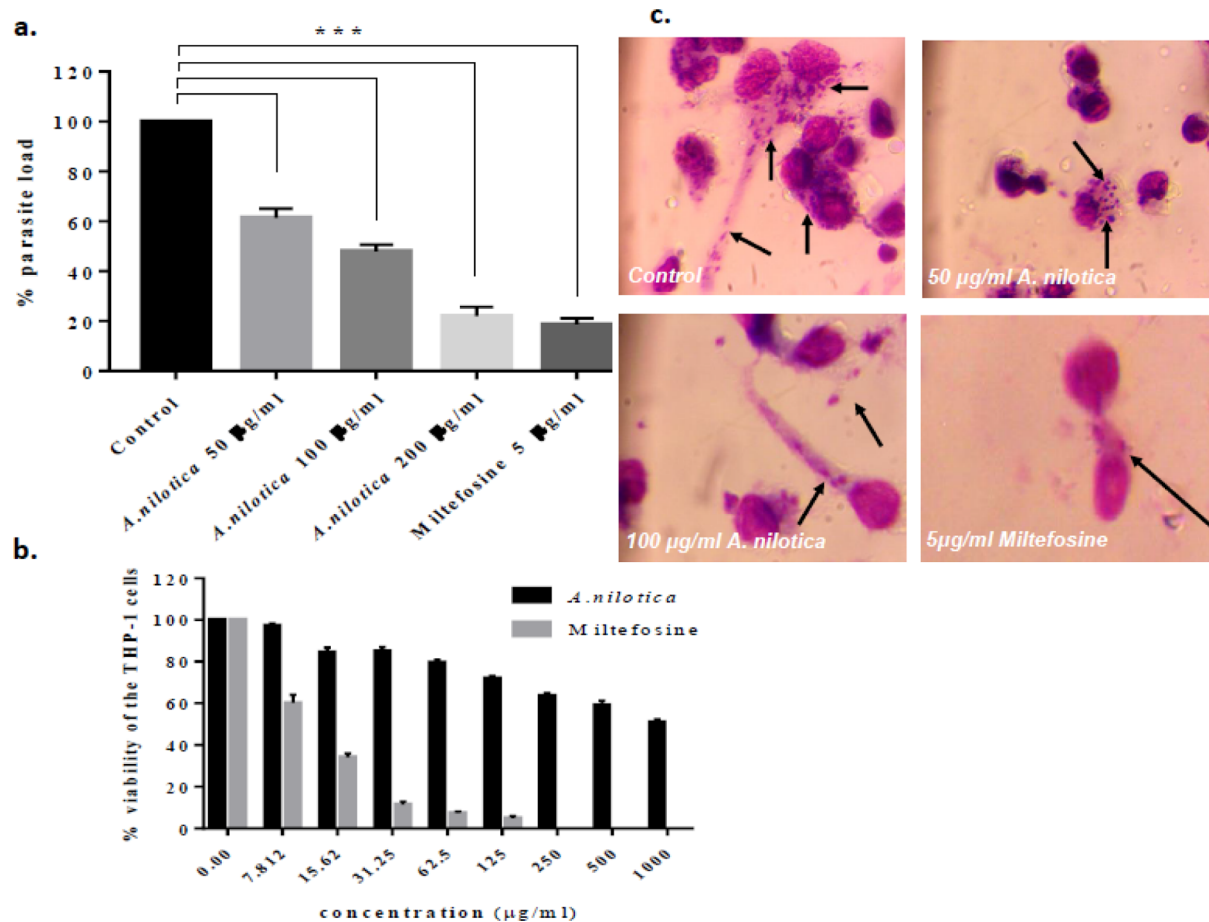


Figure 2. *A. nilotica* bark methanolic extract decreased the intramacrophagic parasites. (a) THP-1-differentiated macrophages were parasitized with 1:10 ratio promastigotes and then treated with different concentrations of the *A. nilotica* fraction. Percent reduction in the parasite load was determined as described in the Materials and Methods. *** $P < 0.001$ value was statistically significant as compared to the control. (b) THP-1-differentiated macrophages were treated with different concentrations of *A. nilotica* and miltefosine (0–1000 $\mu\text{g}/\text{mL}$), and cell viability was ascertained by the MTT assay. (c) Images of Giemsa-stained *L. donovani*-infected macrophages, treated with the extract and control drug. The images were captured at 100 \times under oil immersion. The arrow indicates internalized parasites.

antileishmanial potential of the solvent. After the 4th day of the experimental setup, the culture even in the control and the solvent control gradually decreased because of media exhaustion. The IC_{50} value of *A. nilotica* on *Leishmania* promastigotes was calculated as $19.6 \pm 0.9037 \mu\text{g}/\text{mL}$, and the miltefosine-treated positive control has an IC_{50} of 3.118 ± 0.2395 (Figure 1b). *A. nilotica* treatment exhibits the morphological changes in the promastigote-stage parasites, though at lower doses the parasites retained a normal morphology. At the higher concentrations, there is a reduction in size and shortening of flagella. Miltefosine treatment also exhibited similar morphological changes as extract showed at higher doses (Figure 1c).

2.2. Growth Reversibility Assay after Extract Treatment. *A. nilotica*-treated and -untreated parasites were washed with phosphate-buffered saline after 7 days, and old media were removed and supplemented with fresh media. The samples were further incubated at 22 °C for the next 72 h to study the growth reversibility of parasites. Parasites treated with higher doses do not revert though parasites in flasks of lower dose plant-extract treatment show slower growth reversion (Figure 1d). Suppression of growth reversion was observed significantly ($P < 0.001$) at 250 $\mu\text{g}/\text{mL}$ of *A. nilotica* in comparison to the untreated sample (Figure 1d).

2.3. Cytotoxicity and Antileishmanial Activity of *A. nilotica* on Intramacrophagic Amastigotes. Upon internalization, promastigotes are transformed into the amastigote form inside the parasitophorous vacuoles of macrophages. These amastigote forms of the parasites are nonmotile and define the parasite pathogenicity. Thus, being the biologically and clinically relevant form, it was important to check the antiamastigote efficacy of the *A. nilotica* methanolic extract. THP-1-differentiated macrophages were parasitized by *L. donovani* promastigotes and treated with different doses of the extract. Plant extract treatment reduced the intramacrophagic parasites in a dose-dependent manner with an IC_{50} value of $77.52 \pm 5.167 \mu\text{g}/\text{mL}$ (Figure 2a). Miltefosine was taken as a positive control (Figure 2a). Cell cytotoxicity (CC_{50}) of *A. nilotica* methanolic extract was evaluated along with miltefosine as a positive control on THP-1-differentiated macrophages to study its safe dose. THP-1-differentiated macrophages were incubated with different concentrations of extract/miltefosine (0–1000 $\mu\text{g}/\text{mL}$), and the cell viability was assessed using the 3-(4,5 dimethyl-thiazol-2-yl)-2,5-diphenyl tetrazolium bromide (MTT) assay. It was observed that *A. nilotica* has the least cytotoxic effect on the viability and morphology of the macrophages with a CC_{50} value of $432.7 \pm 7.71 \mu\text{g}/\text{mL}$, while miltefosine showed higher toxicity with a

CC_{50} value of $8.219 \pm 0.6337 \mu\text{g/mL}$ (Figure 2b). A significant reduction in the intramacrophagic parasite count was observed in the micrographs of Giemsa-stained infected and extract-treated macrophages (Figure 2c).

2.4. Thin-Layer Chromatography-Bioautography Identification and GC-MS Analysis of *A. nilotica* Bark Methanolic Extract. Plant secondary metabolites present in *A. nilotica* bark methanolic extract fractions that may have been responsible for the observed antileishmanial effects were identified through thin-layer chromatography (TLC)-bioautography and GC-MS analysis. The total constituents found were 25 (Table 1), out of which the major constituents were 13-docosenoic acid (34.06%), lupeol (20.15%), 9,12-octadecadienoic acid (9.92%), and 6-octadecanoic acid (8.43%).

Table 1. TLC-Bioautography Identification and GC-MS Analysis of *A. nilotica* Bark Methanolic Extract Depicted Key Chemical Constituents of the Extract

S. no.	retention time	% area	compound identified
1.	13.606	0.45	1 <i>H</i> -3 <i>A</i> ,7-methanoazulen-6-ol
2.	14.220	0.79	1 <i>H</i> -benzocycloheptene
3.	14.290	0.32	phenol, 3,5-bis(1,1-dimethylethyl)
4.	15.277	1.49	diethyl phthalate
5.	16.139	0.54	1-(4-isopropylphenyl)-2-methylpropyl acetate
6.	18.855	5.42	hexadecanoic acid, methyl ester
7.	19.328	1.71	N-hexadecanoic acid
8.	20.258	0.30	13-hexyl-oxa-cyclotridec-10-en-2-one
9.	20.465	9.92	9,12-octadecadienoic acid
10.	20.523	8.43	6-octadecenoic acid, methyl ester
11.	20.761	2.81	methyl stearate
12.	20.961	1.44	<i>E,E,Z</i> -1,3,12-nonadecatriene-5,14-diol
13.	22.267	0.17	hexahydro-3-butylphthalide
14.	22.311	2.86	cis-11-eicosenoic acid, methyl ester
15.	22.368	0.53	cis-13-eicosenoic acid, methyl ester
16.	22.527	1.14	eicosanoic acid, methyl ester
17.	23.965	34.06	13-docosenoic acid
18.	24.161	0.84	docosanoic acid
19.	25.532	1.52	cis-15-tetracosensaeure
20.	25.721	0.70	tetracosanoic acid
21.	25.897	0.85	Cyclopentadecanone
22.	27.325	0.34	Octacosane
23.	27.885	0.83	9-octadecenal
24.	33.099	2.36	Stigmasterol
25.	36.679	20.15	Lupeol

2.5. Molecular Docking of *A. nilotica* Methanolic Extract of Major Constituents with the Potential Drug Targets of *L. donovani*. The TR and SMT enzymes were modeled using Modeller 9.24, and the energy minimization was carried out by BIOVIA Discovery Studio. The three-dimensional (3D) cartoon representation of TR and SMT enzymes is shown in Figures S1A and S2A. The models were selected by analyzing their stereochemical quality using the PROCHECK program. The generated models of TR and SMT show a good quality structure having 99.8 and 99% residues in the allowed regions of the Ramachandran plot, respectively (Figures S1B and S2B). The PDBsum tool was used to analyze and found that the 3D structure of the enzyme is composed of mixed α -helices and β -strand ($\alpha + \beta$) secondary structures.²³ The structural topology of TR and SMT showed 5 sheets, 23

strands, 18 helices, and 34 β turns and 2 sheets, 10 strands, 14 helices, and 41 β turns, respectively (Figures S1C,D and S2C,D). Multiple sequence alignments were performed, and Discovery Studio was used to find the key residues and regions around the binding cavity of TR and SMT. The active site residues of the SMT, TR, PTR1, and APRT enzymes making different numbers of hydrogen bonds as well as hydrophobic bonds with the ligands were also identified. Based on binding affinity, lupeol; 9,12-octadecadienoic acid; 6-octadecenoic acid; and 13-docosenoic acid have binding energies of -8.5 , -5.7 , -5.7 , and -5.6 kcal/mol; -8.4 , -4.9 , -4.9 , and -4.7 kcal/mol; -7.9 , -5.3 , -4.4 , and -5.4 kcal/mol; and -6.2 , -6.1 , -5.9 , and -5.9 kcal/mol with SMT, TR, PTR1, and APRT enzymes, respectively (Table 2). The binding pattern of lupeol with SMT, TR, PTR1, and APRT may hinder the substrate accessibility and its subsequent inhibition, as shown in Figures 3–6a, where the binding energies and inhibition constants are -8.5 , -8.4 , -7.9 , and -6.2 kcal/mol and 6.25 , 6.12 , 5.81 , and $4.56 \mu\text{M}$, respectively (Table 2). It shows favorable interactions with SMT through two π -alkyl bonds with Arg347 and Lys351, TR via a π -alkyl bond with Tyr198, PTR1 by two π -alkyl bonds with Val83 and Arg88, and APRT through a hydrogen bond with Thr151 (Figures 3–6b). The binding interaction shown by 9,12-octadecadienoic acid with SMT, TR, PTR1, and APRT may obstruct the substrate accessibility of these proteins, which leads to their subsequent inhibition, as shown in Figures 3–6c, where the binding energies and inhibition constants are -5.7 , -4.9 , -5.3 , and -6.1 kcal/mol and 4.19 , 3.60 , 3.90 , and $4.49 \mu\text{M}$, respectively (Table 2). The favorable interactions are shown by 9,12-octadecadienoic acid with SMT through a hydrogen bond with Lys198, TR via a hydrogen bond with Gly376, and PTR1 by 18 π -alkyl bonds with Phe86, Lys87, Ala90, Ala94, Lys156, Ala157, His160, Arg161, and APRT through a hydrogen bond with Arg82 (Figures 3–6d). The binding pattern of 6-octadecenoic acid with SMT, TR, PTR1, and APRT may lead to their subsequent inhibition by obstructing their substrate accessibility, as shown in Figures 3–6e, where the binding energies and inhibition constants are -5.7 , -4.9 , -4.4 , and -5.9 kcal/mol and 4.19 , 3.60 , 3.24 , and $4.34 \mu\text{M}$, respectively (Table 2).

The important and favorable interactions shown by 6-octadecenoic acid with SMT through two π -alkyl bonds with Lys198, TR via a hydrogen bond with Gly376, PTR1 by a hydrogen bond with Leu92, and APRT through two hydrogen bonds with Arg37 and Arg82 (Figures 3–6f).

The pattern of the interaction of 13-octadecenoic acid with SMT, TR, PTR1, and APRT may lead to their subsequent inhibition by obstructing their substrate accessibility, as shown in Figures 3–6g, where the binding energies and inhibition constants are -5.6 , -4.7 , -5.4 , and -5.9 kcal/mol and 4.12 , 3.46 , 3.97 , and $4.34 \mu\text{M}$, respectively (Table 2). It shows favorable interactions with SMT through two hydrogen bonds with Lys241 and Gln263, TR via a hydrogen bond with Gly376, PTR1 by 20 π -alkyl bonds with Val83, Phe86, Lys87, Ala90, Ala94, Lys156, Ala157, and His160, and APRT through a hydrogen bond with Arg37 and Ar82 (Figures 3–6h).

2.6. Pharmacokinetic Studies of *A. nilotica* Bark Methanolic Extract Constituents. The pharmacological studies were done for the selected ligands against APRT, PTR1, TR, and SMT proteins for a good oral administration established through the Lipinski rule of five,²⁴ which was evaluated by Molsoft L.L.C.: drug-likeness and molecular

Table 2. Molecular Docking Interaction of Abundant Medicinal Constituents of the *A. nilotica* Bark Methanolic Extract Shows Significant Inhibition of *L. donovani* Target Proteins

S. no.	Proteins	Ligands	binding energy (kcal/mol)	pK _{i,pred} (μM)	interacting residues
1.	SMT	Lupeol	-8.5	6.25	Lys198, Tyr206, Met210, Asn215, Pro216, Asn217, Cys240, Gln242, Leu322, Ile344, Arg347, Lys348, Lys351
		9,12-octadecadienoic acid	-5.7	4.19	Lys198, Cys202, Phe203, Tyr206, Met210, Asn215, Asn217, Cys240, Lys241, Phe259, Gln263, Leu322, Ile344, Arg347, Lys348, Lys351
		6-octadecenoic acid	-5.7	4.19	Lys198, Cys202, Phe203, Tyr206, Met210, Asn215, Asn217, Cys240, Lys241, Ala257, Phe259, Ile261, Gln263, Leu322, Ile344, Arg347, Lys348, Lys351
		13-docosenoic acid	-5.6	4.12	Lys198, Gly200, Cys202, Phe203, Tyr206, Met210, Asn215, Pro216, Asn217, Lys241, Phe259, Gln263, Leu322, Ile344, Arg347, Lys348, Lys351
2.	TR	Lupeol	-8.4	6.12	Gly197, Tyr198, Phe230, Val332, Met333, Leu334, His359, Val362, Cys364, Gly374
		9,12-octadecadienoic acid	-4.9	3.60	Tyr198, Phe230, Val332, Met333, Cys364, Gly376
		6-octadecenoic acid,	-4.9	3.60	Gly197, Tyr198, Gly229, Phe230, Val332, Met333, Leu334, Cys362, Cys364, Gly374, Cys375, Gly376
		13-docosenoic acid	-4.7	3.46	Gly197, Tyr198, Phe230, Gly286, Val332, Met333, Leu334, Lys361, Cys362, Cys364, Gly374, Cys375, Gly376
3.	PTR1	Lupeol	-7.9	5.81	His38, Gln63, Ala64, Asp65, Lys71, Ala77, Val83, Lys87, Arg88, Asp91
		9,12-octadecadienoic acid	-5.3	3.90	Phe86, Lys87, Ala90, Ala94, Lys156, Ala157, His160, Arg161
		6-octadecenoic acid	-4.4	3.24	Lys71, Ala77, Val83, Lys87, Arg88, Leu92
		13-docosenoic acid	-5.4	3.97	Val83, Phe86, Lys87, Ala90, Ala94, Lys156, Ala157, His160, Arg161
4.	adenine phosphorybosyl transferase	Lupeol	-6.2	4.56	Pro36, Arg37, Arg82, Lys103, Glu127, Asp146, Ala150, Thr151, Glu152, Gly153, Thr154
		9,12-octadecadienoic acid	-6.1	4.49	Trp29, Arg37, Val39, Pro40, Arg41, Phe42, Ala43, Arg82, Val148, Ala150, Leu176, Ile178, Leu181, Asp206, Leu209
		6-octadecenoic acid	-5.9	4.34	Arg37, Val39, Pro40, Arg41, Phe42, Ala43, Arg82, Val148, Ala150, Leu176, Ile178, Phe180, Leu181, Asp206
		13-docosenoic acid	-5.9	4.34	Arg37, Val39, Pro40, Arg41, Phe42, Ala43, Arg82, Val148, Ala150, Leu176, Ile178, Phe180, Leu181, Asp206, Leu209

property prediction. Lipinski's "rule of five" is an analytical approach for predicting drug-likeness stating that molecules had molecular weight ($MW \leq 500$ Da), high lipophilicity expressed as $\log P$ ($\log P \leq 5$), hydrogen bond donors (HBDs ≤ 5), and hydrogen bond acceptors (HBAs ≤ 10) with good absorption or permeation across the cell membrane. Lupeol, 9,12-octadecadienoic acid, 6-octadecenoic acid, and 13-docosenoic acid followed all the parameters of the Lipinski rule of five, except low lipophilicity, as observed in Table 2. As per the Lipinski rule of five, violation of one parameter is acceptable for an orally active drug. The absorption percentage (AB %) was calculated using the formula.²⁵

$$AB\% = [109 - (0.345 \times TPSA)]$$

It is important to look into the pharmacokinetic properties of the compounds, before animal and clinical studies. To evaluate the biochemical behavior of these compounds inside an organism in respect of absorption, distribution, metabolism, and excretion (ADME), the SwissADME database²⁶ was used to explore the drug-likeness and pharmacokinetic properties of these compounds. The lipophilicity of lupeol, 9,12-octadecadienoic acid, 6-octadecenoic acid, and 13-docosenoic acid showed $\log P_{o/w}$ values of 4.76, 4.61, 4.73, and 5.65, respectively, which indicates high sublingual absorption. Lupeol and 13-docosenoic acid possess low gastrointestinal absorption and poor water-soluble capability, whereas 9,12-octadecadienoic acid and 6-octadecenoic acid show high gastrointestinal absorption as well as moderate water-soluble capability. None of the compounds are permeable to the blood-brain barrier. 9,12-Octadecadienoic acid, 6-octadece-

noc acid, and 13-docosenoic acid are CYP1A2 inhibitors, which are likely to increase the half-life of these compounds and also prevent serious drug interactions. The drug-likeness criteria are qualified by all the ligands with one violation and possess a significant bioavailability score. The results are summarized in Table 3.

The bioactivity prediction of the major constituents of *A. nilotica* bark methanolic extract was analyzed through Molinspiration. The activity was calculated against a G-protein-coupled receptor-ligand, an ion channel modulator, a kinase inhibitor, a nuclear receptor ligand, a protease inhibitor, and an enzyme inhibitor.²⁷ The interpreted values for bioactivity were as follows: active (bioactivity score ≥ 0), moderately active (bioactivity score: between -5.0 and 0.0), and inactive (bioactivity score ≤ -5.0).²⁸ Lupeol, 9,12-octadecadienoic acid, 6-octadecenoic acid, and 13-docosenoic acid were evaluated as active enzyme inhibitors with values 0.52, 0.23, 0.12, and 0.10, respectively. Lupeol and 9,12-octadecadienoic acid were evaluated as active protease inhibitors as well as ion channel modulators (Table 4).

The principal aim of predicting acute toxicity is to evaluate undesirable side effects of a compound after single or multiple exposures to an organism via a known administration route (oral, inhalation, subcutaneous, intravenous, or intraperitoneal). GUSAR was used to determine the acute toxicity of the successfully docked compounds. The parameters used by GUSAR to probe compounds are based on the prediction of activity spectra for substance algorithm and quantitative neighborhoods of atom descriptors. The obtained results were compared with the SYMYX MDL Toxicity Database to

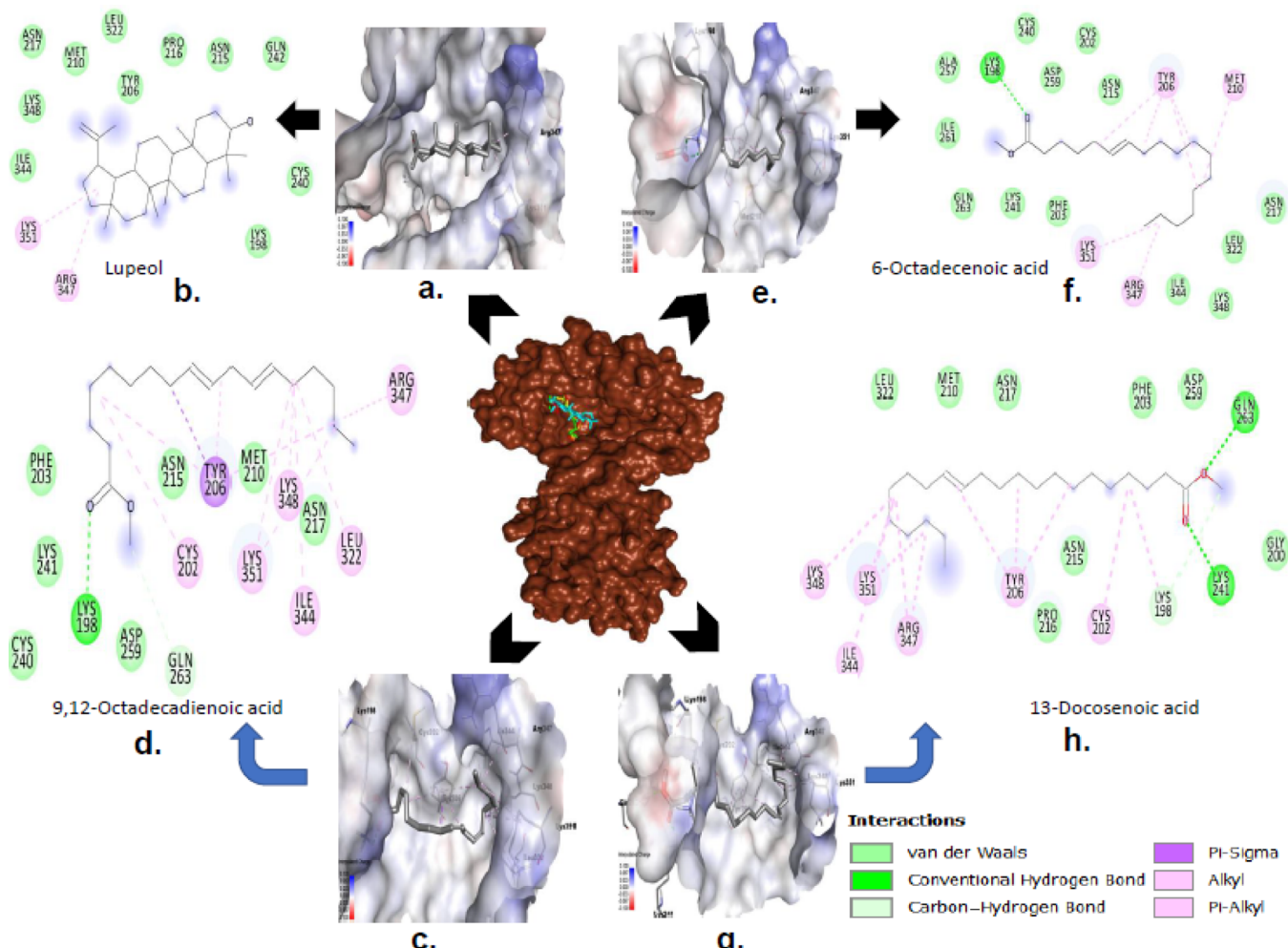


Figure 3. *A. nilotica* major chemical constituents inhibited SMT of *L. donovani* *in silico*. (a) Lupeol blocked the binding pocket of the SMT enzyme. (b) 2D plot showing interactions between the receptor and ligand. (c) 9,12-Octadecadienoic acid blocked the binding pocket of the SMT enzyme. (d) 2D plot showing interactions between the receptor and ligand. (e) 6-Octadecenoic acid blocking the binding pocket of the SMT enzyme. (f) 2D plot showing interactions between the receptor and ligand. (g) 13-Docosenoic acid blocking the binding pocket of the SMT enzyme. (h) 2D plot showing interactions between the receptor and ligand.

further categorize them based on the Organisation for Economic Co-operation and Development (OECD) chemical classification manual.²⁹ The criteria used for these compounds to elicit toxicity are based upon the administration route when the compound dose is more than 7000 mg/kg for an intravenous route, more than 500,000 mg/kg in case of the oral route, and more than 20,000 mg/kg for the intraperitoneal route and subcutaneous database, as shown in Table 5.

3. DISCUSSION

Plant extracts have promising medicinal properties and are extensively used in the traditional system of medicine due to the presence of many active phytoconstituents.³⁰ From the previous studies, it has been revealed that many medicinal plant extracts and their secondary metabolite contents have proven to be efficient and low-toxic antileishmanial drug candidates.^{31,32} *A. nilotica*, which has been identified as potential medicinal plants, is rich in secondary metabolites. Studies based on the GC-MS analysis of *A. nilotica* showed the presence of different types of secondary plant metabolites including polyphenols, mainly composed of condensed tannin and phlobatannin in addition to gallic acid, ellagic acid,

catechin, epigallocatechin-7-gallate, flavonoids, and gum.¹⁵ Different solvent extracts of *A. nilotica* had been shown to have antimicrobial activities including antibacterial, antifungal, antiviral, and antiamoebic.^{20,33,34} We evaluated the antileishmanial potential of *A. nilotica* and identified its secondary metabolite constituents by GC-MS analysis. *A. nilotica* bark methanolic extract inhibited the growth of *L. donovani* promastigotes in a time and dose-dependent manner. It induced morphological changes and a cytoidal mode of parasite killing. The cytoidal mode of the killing of *A. nilotica* maybe because of its richness in phenolic compounds,³⁵ which may cause irreversible changes to the cell membrane.³⁶ Methanolic extract of the fruit of *A. nilotica* had been reported to have antileishmanial activity with an IC₅₀ value of 89.38 µg/mL on the *Leishmania major* promastigotes.³⁷ We determined the IC₅₀ value of *A. nilotica* on *L. donovani* as 19.6 ± 0.9037 µg/mL, which was higher in comparison to the IC₅₀ value of positive control miltefosine (3.118 ± 0.2395 µg/mL). However, the CC₅₀ value of *A. nilotica* on macrophages was determined as 432.7 ± 7.71 µg/mL, while that of the miltefosine was 8.219 ± 0.6337 µg/mL. The plant extract significantly inhibited the growth of the intramacrophagic form

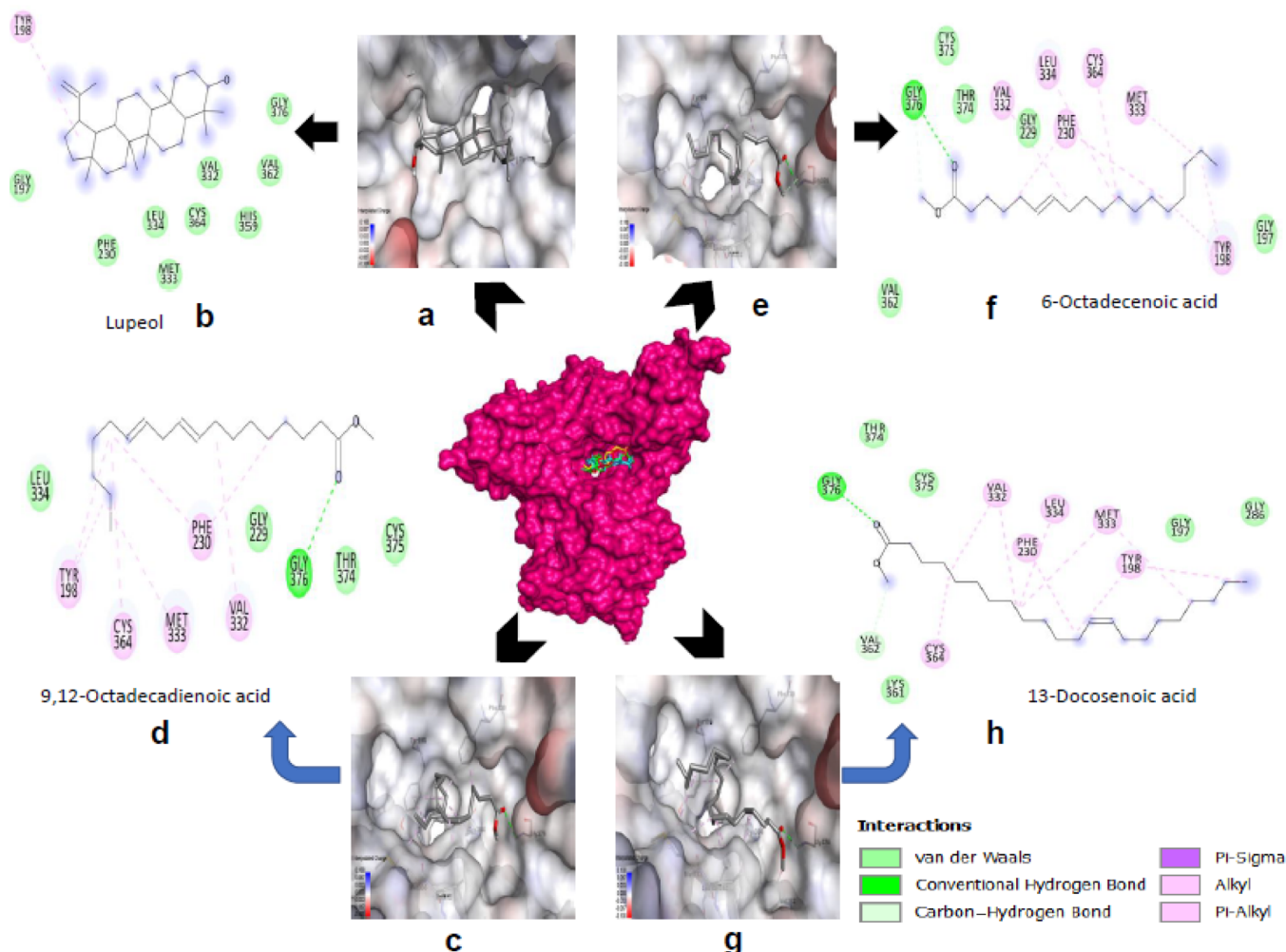


Figure 4. *A. nilotica* major chemical constituents inhibited TR of *L. donovani* *in silico*. (a) Lupeol blocked the binding pocket of the TR enzyme. (b) 2D plot showing interactions between the receptor and ligand. (c) 9,12-Octadecadienoic acid blocked the binding pocket of the TR enzyme. (d) 2D plot showing interactions between the receptor and ligand. (e) 6-Octadecenoic acid blocking the binding pocket of the TR enzyme. (f) 2D plot of 6-octadecenoic acid showing interactions between the receptor and ligand. (g) 13-Docosenoic acid blocked the binding pocket of the TR enzyme. (h) 2D plot showing interactions between the receptor and ligand.

of the parasites. The IC_{50} value of the extract on the amastigote form was calculated as $77.52 \pm 5.167 \mu\text{g/mL}$. *A. nilotica* was found to have low cytotoxicity even after having a higher IC_{50} value as compared to the miltefosine. Therefore, the higher concentration of *A. nilotica* can be used to inhibit the growth of amastigotes inside macrophages. The major constituents identified through GC–MS analysis were 13-docosenoic acid (34.06%), lupeol (20.15%), 9,12-octadecadienoic acid (9.92%), and 6-octadecanoic acid (8.43%). To dissect the mechanism of antileishmanial activity of *A. nilotica*, we further performed the molecular docking study of major constituents of extract identified by GC–MS, with essential enzymes of *Leishmania* including SMT, TR, PTR1, and APRT. These enzymes play an essential role in parasite growth, survival, virulence, and transmission inside the host. SMT is required for the biosynthesis of ergosterol, the major membrane sterol in *L. donovani*.³⁸ The enzyme TR followed the thiol-redox metabolism to keep trypanothione in a reduced form. This antioxidant property of TR is essential for the survival of *L. donovani*.³⁹ PTR1 catalyzed the reduction of conjugated and nonconjugated pterins such as reduced biopterin to dihydrobiopterin.⁴⁰ APRT plays a vital role in the purine

metabolism by converting 6-aminopurines into 6-oxypurines.⁴¹ Molecular docking results proved that lupeol and 9,12-octadecadienoic acid possessed higher binding affinity with SMT, TR, PTR1, and APRT, as shown in Table 2. Pharmacological studies of these selected inhibitors for the Lipinski rule of 5 indicated the violation of only one Lipinski parameter, as shown in Table 3. The pharmacokinetic properties and acute toxicity of lupeol; 9,12-octadecadienoic acid; 6-octadecenoic acid; and 13-docosenoic acid showed a relatively low toxicity profile, which meant the requirement of higher doses to evoke a toxic response. The majority of the compounds were identified as nontoxic chemicals, whereas lupeol was a class 5 chemical with very low toxic effects.⁴² The pharmacokinetic attributes were in favor of these compounds to be exploited as promising antileishmanial drug candidates. The earlier studies had reported that at low concentrations, the ethyl-acetate extract of *A. nilotica* husk induced an increased number of human lymphocyte cell count. This property of the extract may be considered as a human immunity booster.⁴³ Thus, *in vitro*, molecular docking, pharmacokinetic studies, bioactivity scores, and acute toxicity studies suggested possible

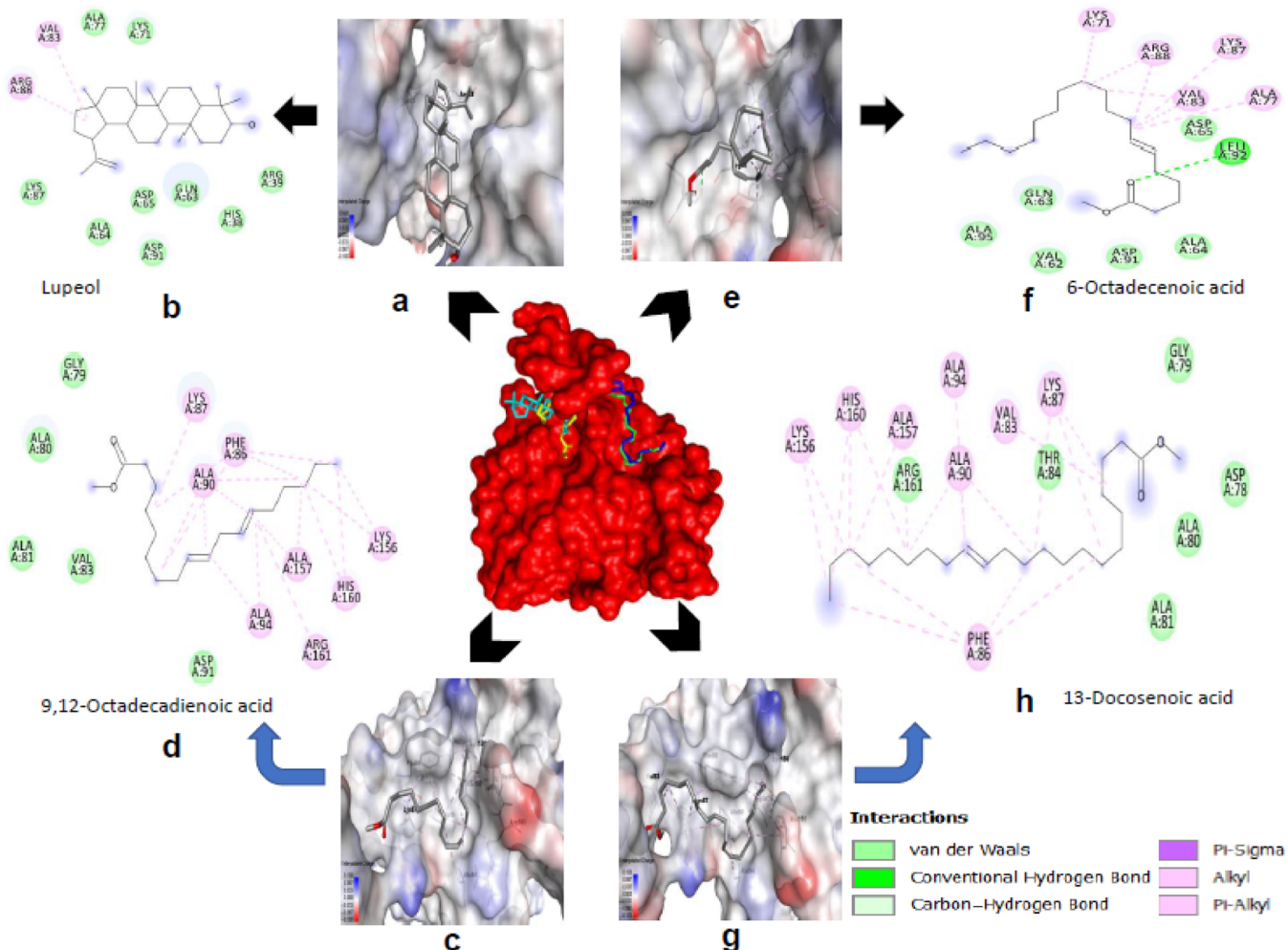


Figure 5. *A. nilotica* major chemical constituents inhibited PTR1 of *L. donovani* *in silico*. (a) Lupeol blocked the binding pocket of the PTR1 (PDB ID: 2XOX) enzyme. (b) 2D plot showing interactions between the receptor and ligand. (c) 9,12-Octadecadienoic acid blocking the binding pocket of the PTR1 (PDB ID: 2XOX) enzyme. (d) 2D plot showing interactions between the receptor and ligand. (e) 6-Octadecenoic acid blocked the binding pocket of the PTR1 (PDB ID: 2XOX) enzyme. (f) 2D plot showing interactions between the receptor and ligand. (g) 13-Docosenoic acid blocked the binding pocket of the PTR1 (PDB ID: 2XOX) enzyme. (h) 2D plot showing interactions between the receptor and ligand.

inhibitory mechanisms of antileishmanial activity of the extract by inhibiting the key enzymes of *Leishmania*.

4. MATERIALS AND METHODS

4.1. Chemicals. M199 media, Roswell Park Memorial Institute (RPMI) 1640 media, penicillin–streptomycin antibiotic cocktail, and fetal bovine serum (FBS) were purchased from Gibco. N-2-Hydroxyethylpiperazine-N'-2-ethanesulfonic acid, sodium bicarbonate, and paraformaldehyde were purchased from Sigma-Aldrich, Saint Louis, MO, USA. Miltefosine, MTT assay reagents, DMSO, and different solvents were procured from Merck & Co., Inc., Kenilworth, NJ, USA. Propidium iodide and the annexin V apoptosis kit were procured from Thermo Scientific. All the other chemicals and reagents were purchased from Sigma-Aldrich, Saint Louis, MO, USA or Merck & Co., Inc., Kenilworth, NJ, USA. unless stated otherwise.

4.2. Parasites and Cell Culture. The infective strain of *L. donovani* (MHOM/IN/83/AG83) was obtained from Dr. Rentala Madhubala (School of Life Science JNU, New Delhi, India). THP-1, a human monocytic cell line, was procured from the Cell Repository of National Centre for Cell Science,

Pune, India. It was further maintained in M199 media. Human monocytic cell line, THP-1, was maintained in RPMI 1640 media supplemented with 10% FBS and 1% penicillin–streptomycin antibiotic medium in a humidified environment at 5% CO₂ and 37 °C temperature. The THP-1 monocytic cell was differentiated to macrophages by using phorbol myristate acetate at a concentration of 20 ng/mL.

4.3. Extract Preparation and Antileishmanial Activity. *A. nilotica* was collected from natural habitats. Bark identification was done at the National Institute of Science Communication and Information Resources (NISCAIR), New Delhi, India. The selected plant material was washed and air-dried in shade at room temperature. The powdered plant materials were soaked in methanol and placed on a rotary shaker at room temperature for 24 h. The extract was filtered and concentrated using a rotatory evaporator under vacuum at 35 °C. The dried plant extract was stored at –20 °C until used for bioassay. To evaluate the antipromastigote potential of *A. nilotica*, stationary phase (2×10^6 cells/mL) promastigotes were incubated with plant extract for 48 h, followed by fixing using 1% paraformaldehyde and counting through a hemocytometer at 22 °C. Miltefosine, a known antileishmanial drug,

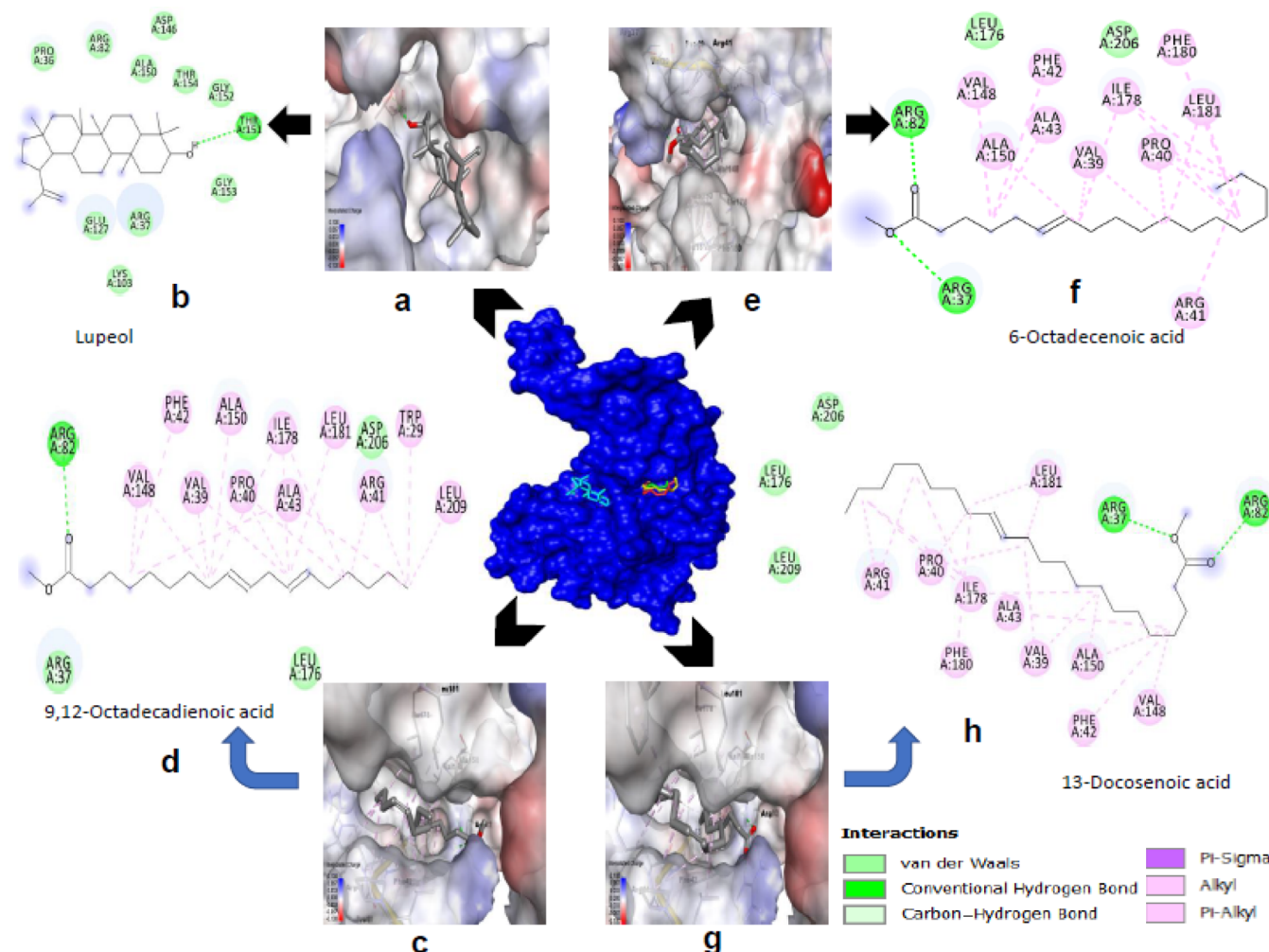


Figure 6. *A. nilotica* major chemical constituents inhibited APRT of *L. donovani* *in silico*. (a) Lupeol blocked the binding pocket of the APRT (PDB ID: 1QB7) enzyme. (b) 2D plot showing interactions between the receptor and ligand. (c) 9,12-Octadecadienoic acid blocked the binding pocket of the APRT (PDB ID: 1QB7) enzyme. (d) 2D plot showing interactions between the receptor and ligand. (e) 6-Octadecenoic acid blocked the binding pocket of the APRT (PDB ID: 1QB7) enzyme. (f) 2D plot showing interactions between the receptor and ligand. (g) 13-Docosenoic acid blocked the binding pocket of the APRT (PDB ID: 1QB7) enzyme. (h) 2D plot showing interactions between the receptor and ligand.

was used as the positive control. Percent viability was determined using the formula

$$\% \text{ viability} = \frac{\text{average parasite count per mL (treated)}}{\text{average parasite count per mL (control)}} \times 100$$

50% inhibitory concentration (IC_{50}) at which parasite growth was reduced by 50% and was assessed by GraphPad Prism 7.00, nonlinear regression curve fit.

4.4. Cytotoxicity Assessment and Antiamastigote Evaluation of Extract. The cytotoxicity of *A. nilotica* on THP-1-differentiated macrophages was assessed by MTT. Briefly, 2×10^6 THP-1 monocytes were seeded in a 96-well tissue culture plate (200 μL /well) in RPMI 1640 complete media for 24 h in an Eppendorf Galaxy 170S CO₂ incubator (Eppendorf India Pvt. Ltd.) at 37 °C and 5% CO₂. After the treatment of THP-1-differentiated macrophages, freshly prepared 5 mg/mL of MTT was added (20 μL /well) with 50 μL of blank media and further incubated for 2–3 h in a CO₂ incubator. Precipitated formazan was dissolved in DMSO; absorbance was recorded at 570 nm in an enzyme-linked

immunosorbent assay plate reader and percent viability was calculated as per the lab's established and published protocol.⁴⁴ To determine the effect of *A. nilotica* on the parasite burden of the host macrophages, 0.5×10^6 THP-1 cells were seeded on the coverslip and placed in the six-well plates in a CO₂ incubator at 37 °C. THP-1 macrophages were plated and infected with *L. donovani* at the ratio of 1:10 (macrophages to *Leishmania*) for 48 h. Then, cells were fixed with chilled methanol and parasite counting was performed under the microscope after Giemsa staining. From the different focus, 100 macrophages were counted to determine the parasite burden of the macrophages. Parasite burden in the infection control was considered 100%, with respect to the parasite load in treated samples.

4.5. GC-MS Analysis of Extract. GC-MS analysis was performed to identify the secondary metabolites that may be responsible for the antileishmanial efficacy of *A. nilotica*. Bark was crushed, powdered, and extracted in methanol and then analyzed on Shimadzu QP2010; GCMS-QP2010 SE: SHIMADZU (Shimadzu Corporation) armed with a DB-5MS column at AIRF, Jawaharlal University, New Delhi, India, as per the established methodology. The mass spectra of the

Table 3. Evaluation of Physico-Chemical and ADMET Properties Shows Feasibility of Usage of the Chemical Constituents for the Treatment of Disease

ligands	MW (<500)	HBD (<5)	HBA (<10)	$\log P_{o/w}$ (lipophilicity)	TPSA (≤140)	absorption percentage (AB %) (>50%)	drug-likeness (Lipinski violations)	GI-absorption	BBB permeant	CYP1A2 inhibitor	bioavailability score	water solubility (log S)
lupeol	426.39	1	1	4.76	20.23	102.02	yes; 1 violation	low	no	no	0.55	-8.64 (poorly soluble)
9,12-octadecadienoic acid	294.48	0	2	4.61	26.30	99.93	yes; 1 violation	high	no	yes	0.55	-4.97 (moderately soluble)
6-octadecenoic acid	296.50	0	2	4.73	26.30	99.93	yes; 1 violation	high	no	yes	0.55	-5.13 (moderately soluble)
13-docosenoic acid	352.60	0	2	5.65	26.30	99.93	yes; 1 violation	low	no	yes	0.55	-6.58 (poorly soluble)

sample were produced in an electron impact ionization mode of 70 eV, and the phytochemicals were identified after the correlation of the recorded mass spectrum with the reference library WILEY8.LIB and NIST14.LIB supplied with the software of the GC–MS system.

4.6. Molecular Docking Studies. To begin with structure-based virtual screening and docking, we used various bioinformatics tools, such as PyRx,⁴⁵ AutoDock Vina,⁴⁶ PyMOL,⁴⁴ and BIOVIA Discovery Studio 2020 pipeline.⁴⁷ The online resources used in the retrieval, analysis, and evaluation of the data are the PubChem database and RCSB Protein Data Bank (PDB).⁴⁸ The target proteins of *L. donovani* and the phytochemical compounds were uploaded into the virtual screening program PyRx. The target protein was changed into a macromolecule, which converted the atomic coordinates into a pdbqt format. Molecular docking was performed by selecting the grid box around the crystal structures, and the rest of the parameters were left as default. AutoDock Vina was used to predict the binding mode and the best binding affinity of the phytochemicals. The algorithm used by AutoDock Vina is a hybrid scoring function that is inspired by X-score, which accounts for hydrogen bonding, hydrophobic effect, van der Waals forces, and deformation penalty. Besides, for computing, the binding energy AutoDock Vina combines both the conformational preferences of the receptor–ligand complex and experimental affinity measurements. The results of molecular docking were screened for binding affinity, and then, all possible docked conformations were generated for different constituents. After analyzing with PyMOL and Discovery Studio, only those conformations were selected which specifically interact with the active-site residues of *L. donovani*-targeted proteins. Discovery Studio was used to analyze detailed interactions and their types including hydrogen bonds, alkyl, π-alkyl, halogen, and the van der Waals interactions formed between different constituents and the target proteins. The most favorable binding poses of the rutin were analyzed by choosing the lowest free energy of binding (ΔG) and the lowest inhibition constant (K_i) which is calculated using the following formula

$$K_{i,\text{pred}} = \text{exponential}^{(\Delta G/RT)}$$

where ΔG is the binding affinity (kcal/mol), R (gas constant) is 1.98 cal K⁻¹ mol⁻¹, and T (room temperature) is 298.15 K.

4.7. Sequence Analysis, Template Identification, Homology Modeling, and Receptor and Ligand Preparation. The protein sequences of TR (XP_003858222.1) and SMT (XP_003865366.1) from *L. donovani* were retrieved from NCBI. The blastP⁴⁹ was performed against Protein Data Bank for the identification of similar templates. The alignment of the query sequences and template sequences was performed using CLUSTAL Ω.⁵⁰ The crystal structure of TR from *Leishmania infantum* 2.95 Å resolution (PDB id: 2JK6_A) and X-ray diffracted crystal structure 1.34 Å resolution (PDB id: SWP4_A) were used as template structures to model the 3D structures of TR and SMT, respectively. PDB was used to retrieve the template structure. Homology modeling was carried out using Modeller 9.24,⁵¹ and PyMol was used for the visualization of the 3D structures. The energy minimization was performed using Discovery Studio. The PROCHECK program and Ramachandran plots were also used for the assessment of the model.²³

Table 4. Bioactivity Prediction of the Selected Ligands against *L. donovani* by Molinspiration

ligands	GPCR ligand	ion channel modulator	kinase inhibitor	nuclear receptor ligand	protease Inhibitor	enzyme inhibitor
lupeol	0.27	0.11	-0.42	0.85	0.15	0.52
9,12-octadecadienoic acid	0.15	0.07	-0.20	0.14	0.03	0.23
6-octadecenoic acid	0.03	-0.03	-0.25	0.06	-0.02	0.12
13-docosenoic acid	0.07	-0.02	-0.17	0.10	0.07	0.10

Table 5. Acute Toxicity Shows the Lethal Dose and Extent of Toxicity of Chemical Constituents on Rodent Models^a

S. no.	Ligands	rat oral LD ₅₀ (mg/kg)	rat IV LD ₅₀ (mg/kg)	rat SC LD ₅₀ (mg/kg)	rat IP LD ₅₀ (mg/kg)	OECD chemical classification
1.	Lupeol	2,888,000	5867	786,900	1,684,000	class 5
2.	9,12-octadecadienoic acid	8,747,000	309,300	9,261,000	4,673,000	non-toxic
3.	6-octadecenoic acid	7,813,000	381,700	7,007,000	3,028,000	non-toxic
4.	13-docosenoic acid	9,279,000	428,600	11,160,000	5,206,000	non-toxic

^aAs per the OECD chemical classification, 9,12-octadecadienoic acid, 6-octadecenoic acid, and 13-docosenoic acid are found to be nontoxic and lupeol is a class 5 chemical.

Crystal structures of the APRT and PTR1 proteins were downloaded from PDB [IDs: 1QB7 (APRT) and 2XO (PTR1)]. The PDB files used for the docking-based virtual screening study were processed by removing water molecules and adding hydrogen atoms. The proteins were finally prepared by Discovery Studio keeping all the parameters at default. The identification of the critical residues of the binding pockets was taken from the native binding pockets of the available crystal structure of proteins, various submitted literature studies, from their homologous template proteins, and investigation in the mechanism of inhibition. The 3D structure of 9,12-octadecadienoic acid, 6-octadecenoic acid, 13-docosenoic acid, and lupeol was retrieved from the PubChem database in an SDF format. The atomic coordinates of all the ligands were changed to a pdbqt setup using Open Babel GUI, an open-source chemical toolbox for the interconversion of chemical structures.⁵² Universal force field was used for the energy minimization.⁵³

4.8. Pharmacokinetic Studies. The selected ligands were evaluated for their pharmacological profiles by analyzing for Lipinski's rule of 5, which was analyzed by Molsoft L.L.C.: drug-likeness and molecular property prediction for drug-likeness (<http://www.molsoft.com/mprop/>). The bioactivity of the selected inhibitors was checked by Molinspiration (<https://molinspiration.com/cgi-bin/properties>). The successfully screened ligands were further evaluated for ADMET (absorption, distribution, metabolism, excretion, and toxicity) properties by GUSAR²⁹ and the SwissADME database.²⁶

ASSOCIATED CONTENT

Supporting Information

The Supporting Information is available free of charge at <https://pubs.acs.org/doi/10.1021/acsomegajournal.1c00366>.

Homology-modeled TR and SMT structures validated through the Ramachandran plot ([PDF](#))

AUTHOR INFORMATION

Corresponding Author

Abdur Rub – *Infection and Immunity Laboratory (414), Department of Biotechnology, Jamia Millia Islamia (A Central University), New Delhi 110025, India; [orcid.org/0000-0003-1301-0761](#); Phone: +91-9560887383; Email: arub@jmi.ac.in*

Authors

Rahat Ali – *Infection and Immunity Laboratory (414), Department of Biotechnology, Jamia Millia Islamia (A Central University), New Delhi 110025, India*

Shams Tabrez – *Infection and Immunity Laboratory (414), Department of Biotechnology, Jamia Millia Islamia (A Central University), New Delhi 110025, India*

Fazlur Rahman – *Infection and Immunity Laboratory (414), Department of Biotechnology, Jamia Millia Islamia (A Central University), New Delhi 110025, India*

Abdulaziz S. Alouffy – *King Abdulaziz City for Science and Technology, Riyadh 12354, Saudi Arabia*

Bader M. Alshehri – *College of Applied Medical Sciences, Majmaah University, Al-Majma'ah 11952, Saudi Arabia*

Fahdah Ayed Alshammari – *College of Sciences and Literature Microbiology, Northern Border University, Arar 73222, Saudi Arabia*

Mohammed A. Alaidarous – *College of Applied Medical Sciences and Deanship of Scientific Research, Majmaah University, Al-Majma'ah 11952, Saudi Arabia*

Saeed Banawas – *College of Applied Medical Sciences and Deanship of Scientific Research, Majmaah University, Al-Majma'ah 11952, Saudi Arabia; Department of Biomedical Sciences, Oregon State University, Corvallis, Oregon 97331, United States*

Abdul Aziz Bin Dukhyil – *College of Applied Medical Sciences, Majmaah University, Al-Majma'ah 11952, Saudi Arabia*

Complete contact information is available at:

<https://pubs.acs.org/10.1021/acsomegajournal.1c00366>

Author Contributions

[¶]R.A., S.T., and F.R. contributed equally.

Funding

The authors would like to thank the Deanship of Scientific Research at Majmaah University, Al Majmaah, 11952, Saudi Arabia, for supporting this work under the Group Project Number RGP-2019-31. The authors are also thankful to the Ministry of Ayush for funding [Z.28015/252/2016-HPC (EMR)-AYUSH-C].

Notes

The authors declare no competing financial interest.

ACKNOWLEDGMENTS

R.A. is thankful to the Ministry of Ayush, GoI for Senior Research Fellowship.

REFERENCES

- (1) Oryan, A.; Akbari, M. Worldwide risk factors in leishmaniasis. *Asian Pac. J. Trop. Med.* **2016**, *9*, 925–932.
- (2) Murray, H. W.; Berman, J. D.; Davies, C. R.; Saravia, N. G. Advances in leishmaniasis. *Lancet* **2005**, *366*, 1561–1577.
- (3) Mamun Huda, M.; Hirve, S.; Siddiqui, N. A.; Malaviya, P.; Banjara, M. R.; Das, P.; Kansal, S.; Gurung, C. K.; Naznin, E.; Rijal, S. Active case detection in national visceral leishmaniasis elimination programs in Bangladesh, India, and Nepal: feasibility, performance and costs. *BMC Public Health* **2012**, *12*, 1001.
- (4) Piscopo, T. V.; Mallia Azzopardi, C. Leishmaniasis. *Postgrad. Med. J.* **2007**, *83*, 649–657.
- (5) Ahmad Kiadalir, A. Global, regional, and national disability-adjusted life-years (DALYs) for 315 diseases and injuries and healthy life expectancy (HALE), 1990–2015: a systematic analysis for the Global Burden of Disease Study 2015. *Lancet* **2016**, *388*, 1603–1658.
- (6) Wang, H.; Naghavi, M.; Allen, C.; Barber, R. M.; Bhutta, Z. A.; Carter, A.; Casey, D. C.; Charlson, F. J.; Chen, A. Z.; Coates, M. M. Global, regional, and national life expectancy, all-cause mortality, and cause-specific mortality for 249 causes of death, 1980–2015: a systematic analysis for the Global Burden of Disease Study 2015. *Lancet* **2016**, *388*, 1459–1544.
- (7) Desjeux, P. The increase in risk factors for leishmaniasis worldwide. *Trans. R. Soc. Trop. Med. Hyg.* **2001**, *95*, 239–243.
- (8) Sundar, S. Drug resistance in Indian visceral leishmaniasis. *Trop. Med. Int. Health* **2001**, *6*, 849–854.
- (9) Chouhan, G.; Islamuddin, M.; Want, M. Y.; Abdin, M. Z.; Ozbak, H. A.; Hemeg, H. A.; Sahal, D.; Afrin, F. Apoptosis mediated leishmanicidal activity of Azadirachta indica bioactive fractions is accompanied by Th1 immunostimulatory potential and therapeutic cure in vivo. *Parasites Vectors* **2015**, *8*, 183.
- (10) Islamuddin, M.; Chouhan, G.; Tyagi, M.; Abdin, M. Z.; Sahal, D.; Afrin, F. Leishmanicidal activities of Artemisia annua leaf essential oil against Visceral Leishmaniasis. *Front. Microbiol.* **2014**, *5*, 626.
- (11) Hill, A. F. Some nomenclatorial problems in Acacia. *Bot. Mus. Leafl., Harv. Univ.* **1940**, *8*, 93–105.
- (12) Bargali, K.; Bargali, S. Acacia nilotica: a multipurpose leguminous plant. *Nat. Sci.* **2009**, *7*, 11–19.
- (13) Leela, V.; Kokila, L.; Lavanya, R.; Saraswathy, A.; Brindha, P. Determination of gallic acid in Acacia nilotica Linn. by HPTLC. *Int. J. Pharm. Technol.* **2010**, *2*, 285–292.
- (14) Singh, B. N.; Singh, B. R.; Singh, R. L.; Prakash, D.; Sarma, B. K.; Singh, H. B. Antioxidant and anti-quorum sensing activities of green pod of Acacia nilotica L. *Food Chem. Toxicol.* **2009**, *47*, 778–786.
- (15) Seigler, D. S. Phytochemistry of Acacia-sensu lato. *Biochem. Syst. Ecol.* **2003**, *31*, 845–873.
- (16) Gilani, S. A.; Khan, A. M.; AleemQureshi, R.; Sherwani, S. K. Ethno-medicinal treatment of common gastrointestinal disorders by indigenous people in Pakistan. *Adv. Biores.* **2014**, *5*, 42–49.
- (17) Al-Fatimi, M.; Wurster, M.; Schröder, G.; Lindequist, U. Antioxidant, antimicrobial and cytotoxic activities of selected medicinal plants from Yemen. *J. Ethnopharmacol.* **2007**, *111*, 657–666.
- (18) Kalaivani, T.; Mathew, L. Free radical scavenging activity from leaves of Acacia nilotica (L.) Wild. ex Delile, an Indian medicinal tree. *Food Chem. Toxicol.* **2010**, *48*, 298–305.
- (19) Eldeen, I. M. S.; Van Staden, J. Antimycobacterial activity of some trees used in South African traditional medicine. *S. Afr. J. Bot.* **2007**, *73*, 248–251.
- (20) Bhargava, A.; Srivastava, A.; Kumbhare, V. Antifungal activity of polyphenolic complex of Acacia nilotica bark. *Indian For.* **1998**, *124*, 292–298.
- (21) Qasim, M.; Abideen, Z.; Adnan, M. Y.; Ansari, R.; Gul, B.; Khan, M. Traditional ethnobotanical uses of medicinal plants from coastal areas. *J. Coastal Life Med.* **2014**, *2*, 22–30.
- (22) Baravkar, A.; Kale, R.; Patil, R.; Sawant, S. J. Pharmaceutical and biological evaluation of formulated cream of methanolic extract of Acacia nilotica leaves. *Res. J. Pharm. Technol.* **2008**, *1*, 480–483.
- (23) Laskowski, R. A.; Rullmann, J. A.; MacArthur, M. W.; Kaptein, R.; Thornton, J. M. AQUA and PROCHECK-NMR: programs for checking the quality of protein structures solved by NMR. *J. Biomol. NMR* **1996**, *8*, 477–486.
- (24) Lipinski, C. A. Lead- and drug-like compounds: the rule-of-five revolution. *Drug Discovery Today: Technol.* **2004**, *1*, 337–341.
- (25) Zhao, Y. H.; Abraham, M. H.; Le, J.; Hersey, A.; Luscombe, C. N.; Beck, G.; Sherborne, B.; Cooper, I. Rate-limited steps of human oral absorption and QSAR studies. *Pharm. Res.* **2002**, *19*, 1446–1457.
- (26) Daina, A.; Michelin, O.; Zoete, V. SwissADME: a free web tool to evaluate pharmacokinetics, drug-likeness and medicinal chemistry friendliness of small molecules. *Sci. Rep.* **2017**, *7*, 42717.
- (27) Mokhnache, K.; Madoui, S.; Khithier, H.; Charef, N. Drug-Likeness and Pharmacokinetics of a bis-Phenolic Ligand: Evaluations by Computational Methods. *Sch. J. Appl. Med. Sci.* **2019**, *1*, 167–173.
- (28) Ungell, A.-L. In Vitro Absorption Studies and Their Relevance to Absorption from the GI Tract. *Drug Dev. Ind. Pharm.* **1997**, *23*, 879–892.
- (29) Lagunin, A.; Zakharov, A.; Filimonov, D.; Poroikov, V. QSAR Modelling of Rat Acute Toxicity on the Basis of PASS Prediction. *Mol. Inf.* **2011**, *30*, 241–250.
- (30) Farnsworth, N. R. The role of ethnopharmacology in drug development. *Ciba Found. Symp.* **1990**, *154*, 2–21.
- (31) Chouhan, G.; Islamuddin, M.; Sahal, D.; Afrin, F. Exploring the role of medicinal plant-based immunomodulators for effective therapy of leishmaniasis. *Front. Immunol.* **2014**, *5*, 193.
- (32) Tahir, A. E.; Ibrahim, A. M.; Satti, G. M. H.; Theander, T. G.; Kharazmi, A.; Khalid, S. A. The potential antileishmanial activity of some Sudanese medicinal plants. *Phytother. Res.* **1998**, *12*, 576–579.
- (33) Rai, S. P.; Prasad, M. S.; Singh, K. Evaluation of the antifungal activity of the potent fraction of hexane extract obtained from the bark of Acacia nilotica. *Int. J. Sci. Res.* **2014**, *3*, 730–738.
- (34) Ambasta, S. P. *The Useful Plants of India*; Publication and Information Directorate, Council of Scientific & Industrial Research: New Delhi, India, 1994.
- (35) Sadiq, M. B.; Hanpitakpong, W.; Tarning, J.; Anal, A. K. Screening of phytochemicals and in vitro evaluation of antibacterial and antioxidant activities of leaves, pods and bark extracts of Acacia nilotica (L.) Del. *Ind. Crops Prod.* **2015**, *77*, 873–882.
- (36) Borges, A.; Ferreira, C.; Saavedra, M. J.; Simões, M. Antibacterial activity and mode of action of ferulic and gallic acids against pathogenic bacteria. *Microb. Drug Resist.* **2013**, *19*, 256–265.
- (37) Fatima, F.; Khalid, A.; Nazar, N.; Abdalla, M.; Mohamed, H.; Toum, A. M.; Magzoub, M.; Ali, M. S. In vitro assessment of anti-cutaneous leishmaniasis activity of some Sudanese plants. *Turkiye Parazitol. Derg.* **2005**, *29*, 3–6.
- (38) Goto, Y.; Bhatia, A.; Raman, V. S.; Vidal, S. E. Z.; Bertholet, S.; Coler, R. N.; Howard, R. F.; Reed, S. G. Leishmania infantum sterol 24-c-methyltransferase formulated with MPL-SE induces cross-protection against L. major infection. *Vaccine* **2009**, *27*, 2884–2890.
- (39) Baiocco, P.; Colotti, G.; Franceschini, S.; Ilari, A. Molecular basis of antimony treatment in leishmaniasis. *J. Med. Chem.* **2009**, *52*, 2603–2612.
- (40) Ong, H. B.; Sienkiewicz, N.; Wyllie, S.; Fairlamb, A. H. Dissecting the metabolic roles of pteridine reductase 1 in Trypanosoma brucei and Leishmania major. *J. Biol. Chem.* **2011**, *286*, 10429–10438.
- (41) Scotti, L.; Ishiki, H.; Mendonca, F. J. B.; Silva, M. S.; Scotti, M. T. In-silico analyses of natural products on leishmania enzyme targets. *Mini-Rev. Med. Chem.* **2015**, *15*, 253–269.
- (42) Mielke, H.; Strickland, J.; Jacobs, M. N.; Mehta, J. M. Biometrical evaluation of the performance of the revised OECD Test

Guideline 402 for assessing acute dermal toxicity. *Regul. Toxicol. Pharmacol.* **2017**, *89*, 26–39.

(43) Al-Bayati, N.; Anwar, S. A.; Mahmood, O. I. Anti leishmanial Activity of Methanolic extract of Juniperus excelsa berries and Acacia nilotica. *Tikret J. Pharm. Sci.* **2016**, *11*, 78–88.

(44) Tabrez, S.; Rahman, F.; Ali, R.; Alouffi, A. S.; Akand, S. K.; Alshehri, B. M.; Alshammari, F. A.; Alam, A.; Alaidarous, M. A.; Banawas, S.; Dukhyil, A. A. B.; Rub, A. Cynaroside inhibits Leishmania donovani UDP-galactopyranose mutase and induces reactive oxygen species to exert antileishmanial response. *Biosci. Rep.* **2021**, *41*, BSR20203857.

(45) Dallakyan, S.; Olson, A. J. Small-molecule library screening by docking with PyRx. *Methods Mol. Biol.* **2015**, *1263*, 243–250.

(46) Trott, O.; Olson, A. J. AutoDock Vina: improving the speed and accuracy of docking with a new scoring function, efficient optimization, and multithreading. *J. Comput. Chem.* **2010**, *31*, 455–461.

(47) Rahman, F.; Tabrez, S.; Ali, R.; Alqahtani, A. S.; Ahmed, M. Z.; Rub, A. Molecular docking analysis of rutin reveals possible inhibition of SARS-CoV-2 vital proteins. *J. Tradit. Complementary Med.* **2021**, *11*, 173.

(48) Kashif, M.; Tabrez, S.; Husein, A.; Arish, M.; Kalaiarasan, P.; Manna, P. P.; Subbarao, N.; Akhter, Y.; Rub, A. Identification of novel inhibitors against UDP-galactopyranose mutase to combat leishmaniasis. *J. Cell. Biochem.* **2018**, *119*, 2653–2665.

(49) Kashif, M.; Hira, S. K.; Upadhyaya, A.; Gupta, U.; Singh, R.; Paladhi, A.; Khan, F. I.; Rub, A.; Manna, P. P. In silico studies and evaluation of antiparasitic role of a novel pyruvate phosphate dikinase inhibitor in Leishmania donovani infected macrophages. *Int. J. Antimicrob. Agents* **2019**, *53*, 508–514.

(50) Zimmermann, L.; Stephens, A.; Nam, S.-Z.; Rau, D.; Kübler, J.; Lozajic, M.; Gabler, F.; Söding, J.; Lupas, A. N.; Alva, V. A Completely Reimplemented MPI Bioinformatics Toolkit with a New HHpred Server at its Core. *J. Mol. Biol.* **2018**, *430*, 2237–2243.

(51) Sali, A.; Blundell, T. L. Comparative protein modelling by satisfaction of spatial restraints. *J. Mol. Biol.* **1993**, *234*, 779–815.

(52) O'Boyle, N. M.; Banck, M.; James, C. A.; Morley, C.; Vandermeersch, T.; Hutchison, G. R. Open Babel: An open chemical toolbox. *J. Cheminf.* **2011**, *3*, 33.

(53) Rappé, A. K.; Casewit, C. J.; Colwell, K. S.; Goddard, W. A., III; Skiff, W. M. UFF, a full periodic table force field for molecular mechanics and molecular dynamics simulations. *J. Am. Chem. Soc.* **1992**, *114*, 10024–10035.